Spherical cell shape of FLC-4 cell, a human hepatoma cell, enhances hepatocyte-specific function and suppresses tumor phenotype through the integration of mRNA–microRNA interaction

Thomas Laurent[1], Yutaro Kataoka[1], Satoru Kobayashi[1], Misaki Ando[1], Seishi Nagamori[2] and Hiroaki Oda[1,*]

[1]Laboratory of Nutritional Biochemistry, Department of Applied Molecular Biosciences, Nagoya University, Nagoya 464-8601, Japan
[2]National Institute of Infectious Diseases, Tokyo 162-8640, Japan
*Author for correspondence (hirooda@agr.nagoya-u.ac.jp)

Biology Open 1, 958–964
doi: 10.1242/bio.20121438
Received 26th March 2012
Accepted 27th June 2012

Summary

The induction mechanism of HNF-4α by spherical cell shape in human hepatoma cells, FLC-4, was investigated. To get insight into the induction mechanism of HNF-4α in three-dimensional FLC-4 cells, mRNA microarray analysis was performed. The gene expression related to drug metabolism and nuclear receptors, such as LXRα, was elevated in spherical FLC-4 cells. We found the first time that the expressions of genes related to malignancy of hepatoma cells, such as HIF-1α, c-Myc and VEGFC, were downregulated by spherical cell shape. Network analysis revealed that HNF-4α would elicit both the enhancement of hepatocyte-specific gene expression and suppression of malignancy. Since HNF-4α gene expression was known to be regulated by microRNA, we inferred that spherical cell shape would induce HNF-4α gene expression through microRNA. To investigate the possibility of such a mechanism, mRNA–microRNA interactions were examined using microRNA microarray and bioinformatics analysis. The level of miR-24, a microRNA targeting HNF-4α, was reduced in spherical FLC-4 cells. On the other hand, spherical cell shape-induced miR-194 and miR-320c would directly downregulate SLC7A5 and E2F1 gene expression, respectively, which are both related to malignancy. Our study suggested that spherical cell shape would induce HNF-4α gene expression and consequent enhancement hepatocyte-specific functions. Spherical cell shape itself would suppress malignancy in FLC-4 cells through microRNA, such as miR-194 and miR-320c.

Key words: Differentiation, Human hepatoma, FLC-4, HNF-4, MicroRNA, Malignancy

Introduction

Three-dimensional culture of rat primary hepatocytes could restore cell polarity and upregulated many liver-specific gene expression including hepatocyte nuclear factor (HNF)-4α, albumin and apo A-I (Oda et al., 1995; Oda et al., 2008). Similarly, three-dimensional culture of human primary hepatocytes could improve the expression levels of drug metabolizing enzymes (Pampaloni et al., 2009). However, long term culture of human primary hepatocytes is difficult to achieve since these cells present limited growth activity and life-span, even in three-dimensional culture (Guillouzo and Guguen-Guillouzo, 2008). To overcome this issue, hepatoma cell lines are commonly used to study liver functions on the long term, though hepatoma cell lines generally lack a substantial set of liver-specific gene expression, especially major cytochrome P-450 (CYP) (Wilkening et al., 2003).

Functional liver cell (FLC) cell lines, human hepatoma cell lines, express and secrete liver-specific proteins at a high level (Hasumura et al., 1988; Homma et al., 1990). Spherical cell shape in FLC-4 cells enhanced liver-specific gene expression, including albumin, apo A-I, CYP3A7, at a similar level to that of human liver (Laurent et al., 2012). However, common hepatoma cell lines did not show higher liver-specific functions in three-dimensional culture (Laurent et al., 2012). We concluded that cell shape *per se*, but not single components of EHS-gel, enhanced this gene expression through HNF-4α, a crucial liver-enriched transcription factor (LETF) regulating a broad range of liver functions (Laurent et al., 2012). Up to now, it is unclear how cell shape induces LETF gene expression.

Recently, microRNA, which are 21–23 nucleotide non-coding RNA, were described as post-transcriptional regulators of gene expression through repressing many specific target mRNA (Ambros, 2004). miR-122, miR-192 and miR-194 are highly expressed in the liver and were shown to regulate liver functions (Girard et al., 2008; Xie et al., 2011). More recently, microRNA–LETF regulatory feedback loops have been found (Takagi et al., 2010; Zeng et al., 2010). In particular, miR-24 was shown to target directly HNF-4α and its downstream target gene expression, such as CYP7A1, in HepG2 cells (Takagi et al., 2010).

In this study, the mechanism of HNF-4α induction by three-dimensional cell shape in FLC-4 cells was explored by performing both mRNA and microRNA microarray analysis and integrating these data by bioinformatics. Gene expression analysis suggested that liver functions were increased and malignant phenotype was repressed in spherical FLC-4 cells. We found that spherical cell shape itself would repress malignancy-related gene expression through microRNA, including miR-194 and miR-320c.

Results and Discussion

Microarray of mRNA revealed that spherical cell shape enhanced drug metabolism and suppressed malignancy in FLC-4 cells

Spherical cell shape of FLC-4 cells on EHS-gel (Fig. 1A) induced HNF-4α gene expression in FLC-4 cells (Fig. 1B). Gene expression of HNF-4α was demonstrated to be regulated by many transcription factors, including LETF (Hatzis and Talianidis, 2001). To understand how spherical cell shape induced HNF-4α gene expression, we performed mRNA microarray and bioinformatics approach. Our results revealed that 83 genes were upregulated, and that 87 genes were downregulated in spherical FLC-4 cells. Various functions were altered by spherical cell shape in FLC-4 cells (Table 1). Among them, gene expression related to drug metabolism was upregulated according to pathway analysis (Table 1). Surprisingly, we found that cancer related gene expression was the most changed by spherical, and was downregulated by spherical cell shape of FLC-4 cells (Table 1).

Spherical cell shape enhanced hepatocyte-specific gene expression in FLC-4 cells

Since drug metabolism was upregulated by spherical cell shape in mRNA microarray (Table 1), we quantified this gene expression using qRT-PCR. Gene expression related to phase I drug metabolizing enzymes (CYP2C9, CYP3A7 and CYP4F2) was elevated in spherical FLC-4 cells (Fig. 1C). CYP2C9 and CYP3A are importantly expressed in the liver (Kamiyama et al., 2007; Rana et al., 2010). Spherical cell shape enhanced the gene expression related to phase II (glutathione S-transferase (GST) A3, sulfotransferase (SULT)1B1, UDP-glucuronosyltransferase (UGT)2B15) and drug efflux pump so-called phase III (ATP-binding cassette (ABC)C2, ABCC3) in FLC-4 cells (Fig. 1C). Drug metabolizing enzyme gene expression, such as CYP2C, CYP3A, SULT and ABCC were shown to be induced by HNF-4α (Kamiyama et al., 2007). We hypothesized that spherical cell shape-dependent induction of HNF-4α would enhance the expressions of drug-metabolizing enzymes in FLC-4 cells.

The gene expression of several nuclear receptors was upregulated in microarray experiment (supplementary material Table S1), especially liver X receptor (LXR)α (NR1H3) (nuclear

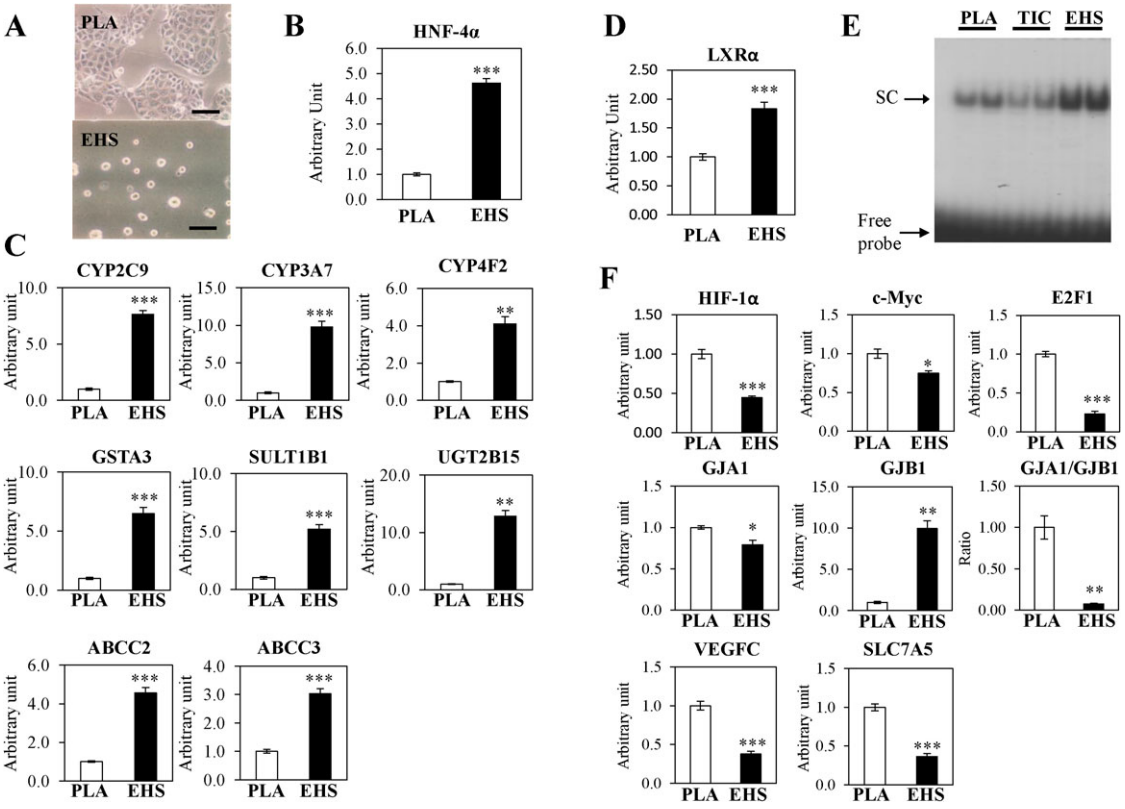

Fig. 1. Hepatocyte-specific gene expression was induced and malignant tumor-related gene expression was suppressed by spherical cell shape in FLC-4 cells. FLC-4 cells were plated at 40% density on uncoated (PLA), EHS-gel-coated (EHS) or type I collagen-coated (TIC) plastic dishes, and cultured for 48 h. Morphological appearance of FLC-4 cells on PLA and EHS-gel (**A**). Scale bar indicates 100 μm. The levels of mRNA for HNF-4α (**B**), drug metabolism-related genes (**C**), LXRα (**D**), and malignant tumor-related genes (**F**) were measured by real-time RT-PCR. The expression was normalized to that of 18S rRNA as a reference for qRT-PCR. Nuclear proteins were extracted and electrophoretic mobility-shift assay (EMSA) was performed using a radiolabeled DR-4 double-stranded oligonucleotide. Specific complex (SC) and free probe are indicated (**E**). Each value is expressed as the mean ± s.e.m for four independent experiments. The statistical significance of differences among values was analyzed by ANOVA and then by Student's t test; *$P < 0.05$, **$P < 0.01$, and ***$P < 0.001$.

Table 1. Top biofunctions and pathways altered in spherical FLC-4 cells in microarray experiment. We compared gene expression between FLC-4 cells cultured on EHS-gel-coated dish or uncoated plastic dish using oligonucleotide microarray.

Category	P value	Upregulated genes	Downregulated genes
Canonical pathway[a]			
Xenobiotic Metabolism Signaling	1.58E−20	21	7
LPS/IL-1 Mediated Inhibition of RXR Function	2.51E−18	21	2
Aryl Hydrocarbon Receptor Signaling	7.94E−17	9	10
Metabolism of Xenobiotics by Cytochrome P450	6.31E−12	14	0
Aldosterone Signaling in Epithelial Cells	2.51E−11	4	11
NRF2-mediated Oxidative Stress Response	2.51E−11	11	5
p53 Signaling	1.10E−10	3	9
Hereditary Breast Cancer Signaling	1.23E−10	3	10
Molecular Mechanisms of Cancer	1.26E−10	6	14
Role of CHK Proteins in Cell Cycle Checkpoint Control	8.13E−10	1	7
Hepatic Cholestasis	8.91E−10	7	6
Biofunctions[b]			
Cancer	4.92E−31	45	61
Cell Death	8.95E−27	31	58
Gastrointestinal Disease	2.55E−22	48	51
Hepatic System Disease	2.55E−22	31	33
Dermatological Diseases and Conditions	2.97E−22	22	39
Cell Cycle	6.31E−21	10	44
Genetic Disorder	5.44E−19	62	63
Respiratory Disease	5.44E−19	14	29
Cellular Growth and Proliferation	1.65E−17	29	51
Tissue Morphology	4.23E−17	21	27
Cellular Development	9.95E−16	21	47
Cellular Movement	6.34E−15	23	31
Hematological Disease	1.06E−14	25	35
Reproductive System Disease	1.44E−14	30	44
Hematological System Development and Function	1.07E−13	20	40
Hematopoiesis	1.37E−13	14	30
Inflammatory Disease	2.47E−13	40	39
Cellular Function and Maintenance	6.19E−13	13	28
Organismal Survival	7.97E−13	20	28

[a]Differentially expressed gene list from microarray experiment were imported in Ingenuity pathway analysis®. Significance expressed as P values were calculated using the right-tailed Fisher's exact test. Canonical pathways significantly changed were obtained ($P < 10^{-8}$).
[b]Differentially expressed gene list from microarray experiment were imported in Ingenuity pathway analysis®. Significance expressed as P values were calculated using the right-tailed Fisher's exact test. Biofunctions significantly changed were obtained ($P < 10^{-12}$).

receptor subfamily 1, group H, member 3) which was the most elevated by spherical cell shape in FLC-4 cells (Fig. 1D; supplementary material Table S1). LXRα is crucial in the maintenance of lipid metabolism (Baranowski, 2008). Hence, we focused on this transcription factor. The DNA-binding activity of LXRα was also increased (Fig. 1E). Our data indicated that spherical cell shape would induce lipid metabolism in FLC-4 cells through LXRα.

Malignancy-related gene expression was downregulated by spherical cell shape in FLC-4 cells

Spherical cell shape suppressed gene expression related to cancer malignant phenotype (Table 1; supplementary material Table S2). Among this gene expression, spherical cell shape suppressed hypoxia-inducible factor (HIF)-1α (Fig. 1F). HIF-1α was reported to induce c-Myc and VEGFC, which are involved in malignancy (Yoo et al., 2011; Zampell et al., 2012). Both c-Myc and VEGFC gene expression was reduced in three-dimensional FLC-4 cells (Fig. 1F). The gene expression of E2F1 (Fig. 1F), a downstream target of c-Myc (Li et al., 2003), was inhibited. HIF-1α and c-Myc were responsible for the shift from oxidative phosphorylation to glycolysis in cancer cell metabolism (Yeung et al., 2008). Hence, spherical cell shape would repress HIF-1α pathway, and consequently would reestablish normal metabolism in FLC-4 cells. Spherical cell shape also reduced solute carrier (SLC)7A5 (LAT1) gene expression, an amino acid transporter implicated in malignancy and cell growth (Fuchs and Bode, 2005) (Fig. 1F). Spherical cell shape decreased significantly the gene expression of gap junction (GJ)A1 (Cx43) and increased GJB1 (Cx32) gene expression, as a result of which the ratio of the gene expression of GJA1/GJB1, a marker of malignancy in hepatoma (Zhang et al., 2007), was downregulated (Fig. 1F). We supposed that spherical cell shape would downregulate malignant phenotype in FLC-4 cells.

Spherical cell shape-dependent induction of HNF-4α would elicit the enhancement of hepatocyte-specific gene expression and suppress malignancy-related gene expression in FLC-4 cells

We speculated that the cell-shape dependent induction of HNF-4α would control the gene expression involved in drug metabolism and lipid metabolism (Table 1; Fig. 1). We hypothesized that cell shape-dependent induction of HNF-4α would be involved in the suppression of HIF-1α, VEGFC, and c-Myc gene expression (Table 1; Fig. 1). Actually, network analysis of mRNA microarray by IPA revealed that HNF-4α played a central role in the induction and suppression of gene expression in spherical FLC-4 cells (Fig. 2). HNF-4α was shown

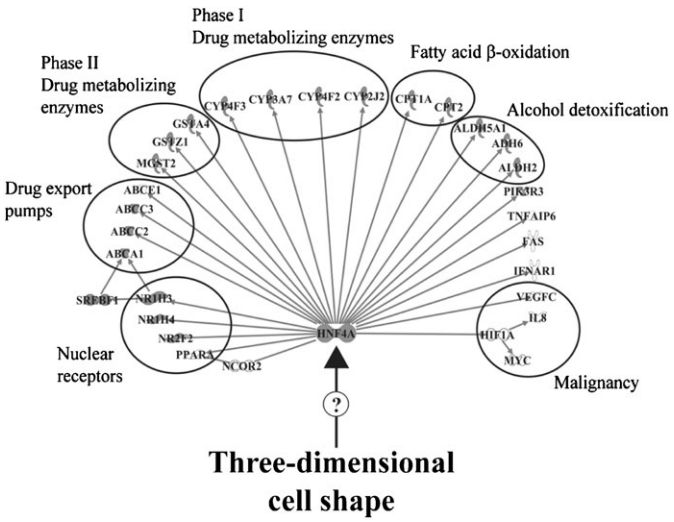

Fig. 2. Hypothetic regulation of gene expression by HNF-4α by spherical cell shape in FLC-4 cells. Focusing on mRNA microarray data, ingenuity pathway analysis (IPA) was used to identify the HNF-4α signaling network in spherical FLC-4. Gray arrows and gray lines indicate regulation of gene expression and protein interactions respectively. Gray and white colors depict upregulation and downregulation of gene expression, respectively. Circles delimitate molecular functions of genes that were classified manually. The gene expression of SREBF1 and HNF4A were measured by real-time RT-PCR.

to repress the gene expression of malignancy-related genes, such as c-Myc and HIF-1α (Wang et al., 2011; Yin et al., 2008). From these results, it was supposed that cell shape-dependent induction of HNF-4α would mediate the induction of liver-specific gene expression and repression of malignancy-related gene expression (Fig. 2).

Changes in microRNA expression would mediate cell shape-dependent induction of HNF-4α and the suppression of malignant phenotype in spherical FLC-4 cells

The purpose of this study was to get insight into the induction mechanism of HNF-4α gene expression by spherical cell shape in FLC-4 cells. To clarify this mechanism, we performed microRNA microarray analysis. The results indicated that 23 microRNA were upregulated, and 6 microRNA were downregulated significantly in spherical FLC-4 cells (Table 2). We then analyzed integrated data of mRNA and microRNA microarray by bioinformatics to get insight into mRNA and microRNA interactions. Although 29 microRNAs were changed by spherical FLC-4 cells on EHS-gel, many of them were not related to changes in mRNAs. And only four microRNAs were selected to be associated with changes in mRNAs (Table 3). Therefore, we focused on these four microRNAs. None of them were not related to HNF-4α.

We also found that miR-24 level was slightly but significantly downregulated (Table 2), which directly suppressed HNF-4α

Table 2. MicroRNA differentially expressed in microRNA microarray experiments[a].

Probe[b]	MicroRNA	Log 2 ratio[c]	FDR[d]
A_25_P00012247	hsa-miR-188-5p	3.42	1.00E−05
A_25_P00010249	hsa-miR-630	3.07	4.20E−04
A_25_P00015036	hsa-miR-320c	2.79	1.00E−05
A_25_P00011703	hcmv-miR-US4	2.59	1.40E−03
A_25_P00014861	hsa-miR-483-5p	2.46	1.00E−05
A_25_P00010800	hsa-miR-663	2.44	4.40E−04
A_25_P00015195	hsa-miR-1268	2.09	1.00E−05
A_25_P00011725	hcmv-miR-UL70-3p	1.91	8.00E−05
A_25_P00015087	hsa-miR-1207-5p	1.76	1.00E−05
A_25_P00010869	hsa-miR-192	1.72	1.00E−05
A_25_P00012230	hsa-miR-134	1.68	1.00E−05
A_25_P00014921	hsa-miR-1225-5p	1.64	8.00E−05
A_25_P00015075	hsa-miR-1202	1.58	1.00E−05
A_25_P00010402	hsa-miR-638	1.53	1.00E−05
A_25_P00015059	hsa-miR-1181	1.49	3.40E−04
A_25_P00015317	hsa-miR-1469	1.26	1.10E−04
A_25_P00012212	hsa-miR-125a-3p	1.23	7.00E−05
A_25_P00011006	hsa-miR-194	1.19	7.00E−05
A_25_P00012698	hsa-miR-455-3p	1.18	2.40E−04
A_25_P00015209	hsa-miR-1275	1.14	7.00E−05
A_25_P00010926	hsa-miR-215	1.09	7.00E−05
A_25_P00012409	hsa-miR-345	1.07	3.00E−05
A_25_P00015286	hsa-miR-1471	1.03	1.34E−03
A_25_P00013116	hsa-let-7b*	−1.06	2.70E−04
A_25_P00014965	hsa-miR-1238	−1.14	3.60E−03
A_25_P00010054	hsa-miR-29b	−1.20	1.10E−04
A_25_P00014887	hsa-miR-513a-5p	−1.79	1.86E−03
A_25_P00013789	ebv-miR-BART19-3p	−2.12	9.10E−04
A_25_P00012257	hsa-miR-193a-3p	−2.70	2.00E−05
A_25_P00010676[e]	hsa-miR-24	−0.39	4.28E−03

*,[a]MicroRNAs were declared significant when log 2 ratio was ≥ 1 or ≤ −1, and False Discovery rate (FDR) was below 0.05.
[b]Agilent Probe IDs are indicated.
[c]Log 2 ratio (FLC-4 cells cultured on EHS-gel-coated dish versus FLC-4 cultured on plastic-coated dish) was calculated from three independent experiments.
[d]FDR was calculated.
[e]miR-24 expression level was indicated though the absolute value of log 2 ratio was below 1.

Table 3. Putative mature microRNA–mRNA regulations in spherical FLC-4 cultured on EHS-gel. FLC-4 cells were plated at 40% density on uncoated or EHS-gel-coated plastic dishes and cultured for 48 hours. Total RNA or total RNA containing small RNA were extracted and submitted to mRNA microarray and microRNA microarray respectively.

Mature miRNA[a]	Entrez gene id	Gene symbol	Description	Fold change[b]
hsa-miR-125a-3p	1871	E2F3	E2F transcription factor 3	2.40
Log ratio: 1.23				
Targets: 139 mRNAs				
hsa-miR-194	8140	SLC7A5	Solute carrier family 7 (cationic amino acid transporter, y+ system), member 5	−1.88
Log ratio: 1.19				
Targets: 258 mRNAs	1871	E2F3	E2F transcription factor 3	2.40
	7026	NR2F2	Nuclear receptor subfamily 2, group F, member 2	2.80
hsa-miR-29b	2941	GSTA4	Glutathione S-transferase A4	1.82
Log ratio: −1.20	1376	CPT2	Carnitine palmitoyltransferase II	1.98
Targets: 850 mRNAs	10437	IFI30	Interferon, gamma-inducible protein 30	1.92
	5295	PIK3R1	Phosphoinositide-3-kinase, regulatory subunit 1 (p85 alpha)	1.90
	9612	NCOR2	Nuclear receptor co-repressor 2	−1.83
	1277	COL1A1	Collagen, type I, alpha 1	−2.00
	3688	ITGB1	Integrin, beta 1 (fibronectin receptor, beta polypeptide, antigen CD29 includes MDF2, MSK12)	−4.11
	8503	PIK3R3	Phosphoinositide-3-kinase, regulatory subunit 3 (p55, gamma)	2.29
	6059	ABCE1	ATP-binding cassette, sub-family E (OABP), member 1	−1.94
	10058	ABCB6	ATP-binding cassette, sub-family B (MDR/TAP), member 6	2.38
hsa-miR-320c	2553	GABPB2	GA binding protein transcription factor, beta subunit 2	−1.84
Log ratio: 2.79				
Targets: 539 mRNAs	1869	E2F1	E2F transcription factor 1	−1.88
	5921	RASA1	RAS p21 protein activator (GTPase activating protein) 1	−2.34
	2935	GSPT1	G1 to S phase transition 1	−1.90
	1871	E2F3	E2F transcription factor 3	2.40
	7048	TGFBR2	Transforming growth factor, beta receptor II (70/80kDa)	2.89
	5295	PIK3R1	Phosphoinositide-3-kinase, regulatory subunit 1 (p85 alpha)	1.90

[a]For mature microRNA differentially expressed in microRNA microarray experiment, log 2 ratio (EHS-gel versus plastic) ($n=3$) and the number of putative target genes are indicated.
[b]Fold change of gene expression is indicated for microRNA targeted genes that were differentially expressed in mRNA microarray experiment.

gene expression (Takagi et al., 2010). Other microRNA predicted to target HNF-4α in Targetscan database were not affected by spherical cell shape. Although the changes in miR-24 might partly explain the induction of HNF-4α by spherical cell shape, we supposed that the change in miR-24 was too small to explain the induction of HNF-4α.

Microarray of mRNA indicated that hepatocyte-specific gene expression, including drug metabolism and insulin signaling, was induced by spherical cell shape in FLC-4 cells (Table 1; supplementary material Table S1). In contrast, malignancy-related gene expression was repressed by spherical cell shape (Table 1; supplementary material Table S2). To understand how microRNA would regulate the gene expression changed by spherical cell shape, we integrated our microRNA and mRNA expression data using Targetscan database to predict mRNA–microRNA interactions. miR-29b was downregulated by spherical cell shape in FLC-4 cells, and was predicted to induce phosphatidylinositol 3-kinase regulatory subunit (PIK3R)1 and PIK3R3 gene expression (Table 3). Since these genes are involved in insulin signaling and malignancy (Anderson, 2010), spherical cell shape-dependent reduction of miR-29b level would regulate these functions in FLC-4 cells. In contrast, miR-194 was upregulated by spherical cell shape, and was predicted to suppress SLC7A5 gene expression, implicated in malignant phenotype (Table 3). These results suggested that spherical cell shape in FLC-4 cells would repress malignancy through miR-194, which was shown to suppress this gene expression in the liver (Meng et al., 2010). Three-dimensional cell shape induced miR-320c, which was predicted to inhibit E2F1 gene expression in FLC-4 cells (Table 3). miR-320 family and E2F1 were shown to inhibit and promote malignant progression respectively (Ladu et al., 2008; Wentz-Hunter and Potashkin, 2011). This indicated that miR-320c would also mediate the suppression of malignancy-related gene expression by spherical cell shape in FLC-4 cells. Based on these results, the enhancement of miR-194 and miR-320c level by spherical cell shape would suppress malignancy in FLC-4 cells.

In conclusion, the present study showed that spherical cell shape in FLC-4 cells greatly induced gene expression related to drug metabolism and lipid metabolism. The suppression of malignancy-related gene expression by spherical cell shape was put into evidence in FLC-4 cells. The induction of HNF-4α gene expression would have a central role in the enhancement of hepatocyte-specific gene expression and the suppression of the

gene expression related to malignancy by spherical cell shape in FLC-4 cells. The integration of microRNA and mRNA microarray data indicated that spherical cell shape would elicit the repression of malignancy through enhancing miR-194 and miR-320c levels.

Materials and Methods

Cell culture

FLC-4 cells were maintained in ASF104 serum-free medium (Ajinomoto Co. Ltd., Tokyo, Japan). Cells were inoculated into 100-mm culture dishes (Corning Inc., Corning, NY, USA) at 40% confluency (number of cells: $2.7\times10^4/cm^2$) and cultured with medium changes every 3 days. Cell cultures were carried out in 100-mm dishes (Cat. no. 1029; Falcon, Becton Dickinson, Lincoln Park, NJ, USA) under a constant temperature of 37℃ with highly humidified 95% air and 5% CO_2. Type I collagen (TIC)-coated dishes were prepared by adding 100 µg/mL TIC (Nitta Gelation, Japan) to plastic dishes (Cat. no. 1029; Falcon, Becton Dickinson, Lincoln Park, NJ, USA). EHS-gel-coated dishes were prepared as described previously (Oda et al., 2008).

Total RNA and small RNA isolation and analysis

Total RNA was extracted according to the method of Chomczynski and Sacchi (Chomczynski and Sacchi, 1987). Total RNA containing small RNAs was extracted from spread FLC-4 cells or spherical FLC-4 cells using the mirVana™ microRNA isolation kit according to the manufacturer's protocol (Cat. #AM1560, Ambion, Austin, TX, USA). Quality of RNA was determined using Bioanalyzer 2100 (Agilent Technologies, Santa Clara, CA, USA) and subsequently quantified using NanoDrop 1000 spectrophotometer (Nanodrop, Wilmington, DE, USA). cDNA was prepared using a High Capacity cDNA Reverse Transcription kit (Cat. #4368814, Applied Biosystems, Foster City, USA) following the manufacturer's instructions. Real-time RT-PCR amplifications were performed in ABI StepOne (Applied Biosystems, Foster City, USA) using 2× Power SYBR Master Mix (Cat. #4309155, Applied Biosystems) as described previously (Laurent et al., 2012). Primer sequences are indicated in supplementary material Table S3. Quantitative RT-PCR melting curve data were collected to check the specificity of PCR. Expression was calculated using the standard curve method. The expression of the chosen genes was normalized to that of 18S rRNA as a reference.

Nuclear protein extraction and electrophoretic mobility-shift assay (EMSA)

Nuclear proteins were extracted from FLC-4 cells and electrophoretic mobility-shift assay (EMSA) was performed as described previously (Laurent et al., 2012). EMSA was performed using the following double-stranded oligonucleotide: DR-4 (5′-agctTCAGGTCACTTCAGGTCAC-3′, 5′-tcgaGTGACCTGAAGTGACCT-GA-3′).

Microarray of mRNA and data analysis

Total RNA from spread and spherical FLC-4 cells were used for mRNA microarray analysis. We utilized a DNA oligonucleotide microarray containing duplicate cDNA spots of 1262 well annotated genes of various functional classes, including cytokines/growth factors and their receptors, oncogenes, drug metabolizing enzyme, transcription factors and housekeeping genes (Hitachi Life Science, Saitama, Japan). Five micrograms of total RNA isolated was *in vitro* amplified, and the antisense RNA (aRNA) from spread FLC-4 cells was labeled with a fluorescent dye Cy5, while aRNA from spherical FLC-4 cells was labeled with Cy3. The arrays were hybridized at 62℃ for 10 h in the hybridization buffer containing equal amounts of Cy3- or Cy5-labeled cDNA, and they were then scanned by the ScanArray 5000 scanner (GSI Lumonics, Boston, MA, USA). The data were analyzed by using the QuantArray software (GSI Lumonics, Boston, MA, USA). The average of fluorescence intensities of duplicate spots was obtained after global normalization between Cy3 and Cy5 signals. Genes were considered as differentially expressed when fold change was above 1.8 or below −1.8 and $P < 0.05$. List of differentially expressed genes was imported in IPA (Ingenuity Systems, Redwood City, CA, USA), and no filter criterion was used for this analysis. Network analysis and biofunction analysis were performed using the IPA software.

MicroRNA microarray and data analysis

200 ng of total RNA from FLC-4 cells cultured on EHS-gel or plastic dishes for 48 hours ($n=3$) were labeled using the miRNA Complete Labeling and Hybridization Kit (Cat. #5190-0456, Agilent, Santa Clara, CA, USA). Labeled RNA was hybridized in Agilent Human microRNA Microarray V3 for 20 h at 20 rpm, 55℃ (Cat. #G4470C, Agilent, Santa Clara, CA, USA). Slides were washed and scanned according to the manufacturer's instructions. Images were quantified using Feature Extraction (Agilent, Santa Clara, CA, USA). The miRNA array contained the complete content sourced from Sanger database 12.0, i.e. 851 probes for human and 88 probes for viral miRNA transcripts (Agilent, Santa Clara, CA, USA). The raw dataset was normalized and analyzed using the "AgiMicroRna" package of the Bioconductor (http://www.bioconductor.org) suite of software for the R statistical programming language (http://www.r-project.org). Quantile normalization was then used to standardize the data across arrays, and a linear model was fitted to each microRNA using "AgiMicroRna" package. The resultant P values were obtained using a moderated t-test statistics, adjusted for multiple testing by using the Benjamini–Hochberg correction of the false-discovery rate. MicroRNA were selected according to the following criteria: False Discovery Rate (FDR) < 0.05. The results are expressed in log 2 ratio (EHS-gel versus plastic). MicroRNA were selected according to the following criteria: log 2 ratio ≤ -1 or log 2 ratio ≥ 1. The miRNA target prediction was performed using TargetScan database (http://www.targetscan.org).

Statistical analysis

The significance of differences among values was analyzed by ANOVA and Student's t-test. When P value was below 0.05, differences were considered significant. Values in the text are expressed as means ± s.e.m.

Acknowledgements

We are grateful to Yasuko Matsuyama for technical assistance.

Competing Interests

The authors have no competing interests to declare.

References

Ambros, V. (2004). The functions of animal microRNAs. *Nature* **431**, 350-355.

Anderson, D. H. (2010). p85 plays a critical role in controlling flux through the PI3K/PTEN signaling axis through dual regulation of both p110 (PI3K) and PTEN. *Cell Cycle* **9**, 2055-2056.

Baranowski, M. (2008). Biological role of liver X receptors. *J. Physiol. Pharmacol.* **59 Suppl 7**, 31-55.

Chomczynski, P. and Sacchi, N. (1987). Single-step method of RNA isolation by acid guanidinium thiocyanate-phenol-chloroform extraction. *Anal. Biochem.* **162**, 156-159.

Fuchs, B. C. and Bode, B. P. (2005). Amino acid transporters ASCT2 and LAT1 in cancer: partners in crime? *Semin. Cancer Biol.* **15**, 254-266.

Girard, M., Jacquemin, E., Munnich, A., Lyonnet, S. and Henrion-Caude, A. (2008). miR-122, a paradigm for the role of microRNAs in the liver. *J. Hepatol.* **48**, 648-656.

Guillouzo, A. and Guguen-Guillouzo, C. (2008). Evolving concepts in liver tissue modeling and implications for *in vitro* toxicology. *Expert Opin. Drug Metab. Toxicol.* **4**, 1279-1294.

Hasumura, S., Nagamori, S., Fujise, K., Homma, S., Sujino, H., Matsuura, T., Shimizu, K., Niiya, M., Kameda, H., Satomi, N. et al. (1988). Effects of TNF on human hepatocellular carcinoma cell lines and their modification by hyperthermia. *Hum. Cell* **1**, 238-244.

Hatzis, P. and Talianidis, I. (2001). Regulatory mechanisms controlling human hepatocyte nuclear factor 4alpha gene expression. *Mol. Cell. Biol.* **21**, 7320-7330.

Homma, S., Nagamori, S., Fujise, K., Hasumura, S., Sujino, H., Matsuura, T., Shimizu, K., Niiya, M. and Kameda, H. (1990). Establishment and characterization of a human hepatocellular carcinoma cell line JHH-7 producing alpha -fetoprotein and carcinoembryonic antigen—changes in secretion of AFP and CEA from JHH-7 cells after heat treatment. *Hum. Cell* **3**, 152-157.

Kamiyama, Y., Matsubara, T., Yoshinari, K., Nagata, K., Kamimura, H. and Yamazoe, Y. (2007). Role of human hepatocyte nuclear factor 4alpha in the expression of drug-metabolizing enzymes and transporters in human hepatocytes assessed by use of small interfering RNA. *Drug Metab. Pharmacokinet.* **22**, 287-298.

Ladu, S., Calvisi, D. F., Conner, E. A., Farina, M., Factor, V. M. and Thorgeirsson, S. S. (2008). E2F1 inhibits c-Myc-driven apoptosis via PIK3CA/Akt/mTOR and COX-2 in a mouse model of human liver cancer. *Gastroenterology* **135**, 1322-1332.

Laurent, T., Murase, D., Tsukioka, S., Matsuura, T., Nagamori, S. and Oda, H. (2012). A novel human hepatoma cell line, FLC-4, exhibits highly enhanced liver differentiation functions through the three-dimensional cell shape. *J. Cell. Physiol.* **227**, 2898-2906.

Li, Z., Van Calcar, S., Qu, C., Cavenee, W. K., Zhang, M. Q. and Ren, B. (2003). A global transcriptional regulatory role for c-Myc in Burkitt's lymphoma cells. *Proc. Natl. Acad. Sci. USA* **100**, 8164-8169.

Meng, Z., Fu, X., Chen, X., Zeng, S., Tian, Y., Jove, R., Xu, R. and Huang, W. (2010). miR-194 is a marker of hepatic epithelial cells and suppresses metastasis of liver cancer cells in mice. *Hepatology* **52**, 2148-2157.

Oda, H., Nozawa, K., Hitomi, Y. and Kakinuma, A. (1995). Laminin-rich extracellular matrix maintains high level of hepatocyte nuclear factor 4 in rat hepatocyte culture. *Biochem. Biophys. Res. Commun.* **212**, 800-805.

Oda, H., Yoshida, Y., Kawamura, A. and Kakinuma, A. (2008). Cell shape, cell-cell contact, cell-extracellular matrix contact and cell polarity are all required for the maximum induction of CYP2B1 and CYP2B2 gene expression by phenobarbital in adult rat cultured hepatocytes. *Biochem. Pharmacol.* **75**, 1209-1217.

Pampaloni, F., Stelzer, E. H. and Masotti, A. (2009). Three-dimensional tissue models for drug discovery and toxicology. *Recent Pat. Biotechnol.* **3**, 103-117.

Rana, R., Chen, Y., Ferguson, S. S., Kissling, G. E., Surapureddi, S. and Goldstein, J. A. (2010). Hepatocyte nuclear factor 4alpha regulates rifampicin-mediated induction of CYP2C genes in primary cultures of human hepatocytes. *Drug Metab. Dispos.* **38**, 591-599.

Takagi, S., Nakajima, M., Kida, K., Yamaura, Y., Fukami, T. and Yokoi, T. (2010). MicroRNAs regulate human hepatocyte nuclear factor 4alpha, modulating the expression of metabolic enzymes and cell cycle. *J. Biol. Chem.* **285**, 4415-4422.

Wang, Z., Bishop, E. P. and Burke, P. A. (2011). Expression profile analysis of the inflammatory response regulated by hepatocyte nuclear factor 4α. *BMC Genomics* **12**, 128.

Wentz-Hunter, K. K. and Potashkin, J. A. (2011). The role of miRNAs as key regulators in the neoplastic microenvironment. *Mol. Biol. Int.* **2011**, 839872.

Wilkening, S., Stahl, F. and Bader, A. (2003). Comparison of primary human hepatocytes and hepatoma cell line Hepg2 with regard to their biotransformation properties. *Drug Metab. Dispos.* **31**, 1035-1042.

Xie, Q. H., He, X. X., Chang, Y., Sun, S. Z., Jiang, X., Li, P. Y. and Lin, J. S. (2011). MiR-192 inhibits nucleotide excision repair by targeting ERCC3 and ERCC4 in HepG2.2.15 cells. *Biochem. Biophys. Res. Commun.* **410**, 440-445.

Yeung, S. J., Pan, J. and Lee, M. H. (2008). Roles of p53, MYC and HIF-1 in regulating glycolysis - the seventh hallmark of cancer. *Cell. Mol. Life Sci.* **65**, 3981-3999.

Yin, C., Lin, Y., Zhang, X., Chen, Y. X., Zeng, X., Yue, H. Y., Hou, J. L., Deng, X., Zhang, J. P., Han, Z. G. et al. (2008). Differentiation therapy of hepatocellular carcinoma in mice with recombinant adenovirus carrying hepatocyte nuclear factor-4alpha gene. *Hepatology* **48**, 1528-1539.

Yoo, Y. G., Christensen, J. and Huang, L. E. (2011). HIF-1α confers aggressive malignant traits on human tumor cells independent of its canonical transcriptional function. *Cancer Res.* **71**, 1244-1252.

Zampell, J. C., Yan, A., Avraham, T., Daluvoy, S., Weitman, E. S. and Mehrara, B. J. (2012). HIF-1α coordinates lymphangiogenesis during wound healing and in response to inflammation. *FASEB J.* **26**, 1027-1039.

Zeng, C., Wang, R., Li, D., Lin, X. J., Wei, Q. K., Yuan, Y., Wang, Q., Chen, W. and Zhuang, S. M. (2010). A novel GSK-3 beta-C/EBP alpha-miR-122-insulin-like growth factor 1 receptor regulatory circuitry in human hepatocellular carcinoma. *Hepatology* **52**, 1702-1712.

Zhang, D., Kaneda, M., Nakahama, K., Arii, S. and Morita, I. (2007). Connexin 43 expression promotes malignancy of HuH7 hepatocellular carcinoma cells via the inhibition of cell-cell communication. *Cancer Lett.* **252**, 208-215.